

Protoneutron Stars with Kaon Condensation and their Delayed Collapse

Masatomi Yasuhira and Toshitaka Tatsumi

Department of Physics, Kyoto University, JAPAN

e-mail: yasuhira@ruby.scphys.kyoto-u.ac.jp

tatsumi@ruby.scphys.kyoto-u.ac.jp

abstract

Properties of protoneutron stars are discussed in the context of kaon condensation. Thermal and neutrino trapping effects are very important ingredients to study them. By solving the TOV equation, we discuss the static properties of protoneutron stars and the possibility of the delayed collapse during their evolution.

1 Introduction

Protoneutron stars (PNS), which are formed after the gravitational collapse of massive stars, consist of hot and dense hadronic matter. At birth matter is lepton rich due to the trapping of neutrinos and has entropy per baryon of order 1-3 in units of Boltzmann constant. PNS evolve in a few tens of seconds through the deleptonization and initial cooling stages to usual cold neutron stars[1]. During the evolution, some of them may become to be gravitationally unstable due to some hadronic phase transitions and collapse to the low-mass black holes[2], which we call the delayed collapse.

To make the low-mass black holes with the gravitational mass of $O(1.4M_{\odot})$, first, the maximum mass of neutron stars must be sufficiently low and secondly mass of PNS must exceed the maximum mass during their evolution due to neutrino emission, cooling and/or fall-back of matter. The possibility of making the low-mass black holes in supernovae and its relation with SN1987A has been discussed by many authors [3][4][5]. The observation of neutrinos from SN1987A suggested a formation of a PNS in it. However the neutron star has never been detected so far. One idea to resolve this mystery is that the neutron star must have collapsed further into a low-mass black hole at some later time because of either the accretion of a sufficient fall-back mass and/or some change of its equation of state(EOS)

Thus it is very important to study the change of EOS during the evolution of PNS to discuss the possibility of the delayed collapse: EOS depends on what kind of hadronic phase transitions takes place: quark matter, boson condensed matter, hyperonic matter and so on. There neutrino-trapping and thermal effects play an important role in the rearrangement of constituents of matter and they are also crucial for whether phase transition occurs or not. Simulations to describe the evolution of PNS and the delayed collapse have been done[6][7][8]. In this paper we study kaon condensation in hot and neutrino-trapping matter, which may be a key object of the delayed collapse due to the large softening of EOS.

Kaon condensation was first suggested by Kaplan and Nelson[9] and has been studied by many authors mainly at zero temperature[10]. Its implications have been discussed mainly in the context of cold neutron stars; maximum mass, cooling mechanism, rapidly rotating pulsars and so on. Recently we have presented a formulation to treat thermal and quantum fluctuations around the condensate on the basis of chiral symmetry [11][12][13]. Making full use of the group structure of chiral manifold, we have derived the thermodynamic potential from the nonlinear chiral Lagrangian. The Goldstone mode arises from the V-spin symmetry breaking there. We have found the dispersion relation for this mode, and found that it plays an important role at finite temperature.

Baumgarte et al. performed a numerical simulation of the evolution of PNS by taking into account the change of EOS due to kaon condensation and examined how they collapse to black holes[6]. However they used the EOS of kaon condensed matter at zero temperature. Pons et al. also discussed the EOS of kaon condensed matter with meson exchange model and PNS [14]. They conclude the thermal effects is a key object to the delayed collapse. However, here we study the kaon condensation based on chiral symmetry and find that the delayed collapse is caused not by the thermal effect in the cooling era but by the neutrino-trapping effect in the deleptonization era.

In Sect.2 we briefly review the essential part of the formulation that enables us to treat thermal and quantum fluctuations around the condensate transparently.

In Sect.3 we discuss the properties of EOS and PNS and especially the possibility of the delayed collapse.

Summary and concluding remarks are given in Sect.4.

2 Formulation

Recently we have presented a framework to take into account the quantum and/or thermal fluctuations around the condensate, in accordance with chiral symmetry [11][12][13]. The effective partition function Z_{chiral} at temperature T can be written as

$$Z_{chiral} = N \int [dU][dB][d\bar{B}] \exp \left[\int_0^\beta d\tau \int d^3x \{ \mathcal{L}_{chiral}(U, B) + \delta\mathcal{L}(U, B) \} \right], \quad (1)$$

with the imaginary time $\tau = it$ and $\beta = 1/T$. $\mathcal{L}_{chiral}(U, B) = \mathcal{L}_0(U, B) + \mathcal{L}_{SB}(U, B)$ is the Kaplan Nelson Lagrangian[9] and is represented with the octet baryon field, B , and the chiral field, $U = \exp[2iT_a\phi_a/f] \in SU(3)$, with $SU(3)$ generators T_a and the Goldstone fields ϕ_a . $\delta\mathcal{L}$ is the induced SB term as a result of introduction of chemical potentials, μ_K and μ_n ,

$$\begin{aligned} \delta\mathcal{L} = & -\frac{f^2\mu_K}{4} \text{tr}\{[T_{em}, U] \frac{\partial U^\dagger}{\partial \tau} + \frac{\partial U}{\partial \tau} [T_{em}, U^\dagger]\} \\ & -\frac{\mu_K}{2} \text{tr}\{B^\dagger[(\xi^\dagger[T_{em}, \xi] + \xi[T_{em}, \xi^\dagger]), B]\} \\ & -\frac{f^2\mu_K^2}{4} \text{tr}\{[T_{em}, U][T_{em}, U^\dagger]\} + \mu_n \text{tr}\{B^\dagger B\} - \mu_K \text{tr}\{B^\dagger [T_{em}, B]\} \end{aligned} \quad (2)$$

with $U = \xi^2$. Generally it is complicated to perform the path integral by separating the fields ϕ_a into the sum of classical fields $\langle\phi_a\rangle$ and fluctuation fields $\tilde{\phi}_a$ in the standard way, because $\{\phi_a\}$ reside on the curved manifold $SU(3) \times SU(3)/SU(3)$. Instead, we introduce the local coordinates around the condensed point to eliminate the curvature effect in the neighborhood, which is equivalent to the following parametrization for U ;

$$U = \zeta U_f \zeta (\xi = \zeta U_f^{1/2} u^\dagger = u U_f^{1/2} \zeta), \quad \zeta = \exp(\sqrt{2}i\langle M \rangle/f), \quad (3)$$

where $\langle M \rangle$ represents the condensate, $\langle M \rangle = V_+ \langle K^+ \rangle + V_- \langle K^- \rangle$, with $K^\pm = (\phi_4 \pm i\phi_5)/\sqrt{2}$ and $\theta^2 \equiv 2K^+ K^-/f^2$, while $U_f = \exp[2iT_a\phi_a/f]$ means the fluctuation field. It may be interesting to see that this procedure can be also regarded as the separation of the zero-mode [15].

Accordingly, defining a new baryon field B' by way of

$$B' = u^\dagger B u, \quad (4)$$

we can see eventually that

$$\mathcal{L}_{chiral}(U, B) = \mathcal{L}_0(U_f, B') + \mathcal{L}_{SB}(\zeta U_f \zeta, u B' u^\dagger), \quad \delta \mathcal{L}(U, B) = \delta \mathcal{L}(\zeta U_f \zeta, u B' u^\dagger). \quad (5)$$

Thus only the SB terms *prescribe* the KN dynamics in the condensed phase; we can easily see that the KN sigma terms, $\Sigma_{Ki}(i = n, p)$, stem from \mathcal{L}_{SB} , while the Toozawa-Weinberg term from $\delta \mathcal{L}$ [11][13].

The integration measure is properly approximated as $[dU_f] \simeq \prod_{a=1}^8 [d\phi_a]$ in the neighborhood of the condensate and finally we find

$$Z_{chiral} \simeq \int \prod_{a=1}^8 [d\phi_a] [dB'] [d\bar{B}'] \exp \left[\int_0^\beta d\tau \int d^3x \mathcal{L}_{chiral}^{eff}(\zeta, U_f, B') \right], \quad (6)$$

with the effective chiral Lagrangian, $\mathcal{L}_{chiral}^{eff}(\zeta, U_f, B') = \mathcal{L}_0(U_f, B') + \mathcal{L}_{SB}(\zeta U_f \zeta, u B' u^\dagger) + \delta \mathcal{L}(\zeta U_f \zeta, u B' u^\dagger)$.

We then evaluate the partition function Z_{chiral} up to the one-loop level under the Hartree approximation for kaon-nucleon interactions; we need not care about the nucleon loops in the heavy baryon limit (HBL), which we hereafter use in this paper.

During this course, the poles of the thermal Green function for kaons give the excitation spectra of kaonic modes with energies (E_\pm). The mode with E_- is the Goldstone mode and exhibits the Bogoliubov spectrum, which stems from the spontaneous breaking of V -spin symmetry in the condensed phase. It gives a large contribution to the thermodynamic quantities through the Bose-Einstein distribution function. Under the relevant approximation, they are reduced to the simple form

$$E_\pm(\mathbf{p}) \simeq \sqrt{p^2 + \cos\langle\theta\rangle m_K^{*2} + b^2} \pm (b + \cos\langle\theta\rangle \mu_K). \quad (7)$$

We use this form in the following calculations. We have discussed its relevance in the previous papers[13] and have seen its practical usefulness in giving the thermodynamic quantities.

Eventually the effective themodynamical potential $\Omega_{chiral} = -T \ln Z_{chiral}$ reads

$$\Omega_{chiral} = \Omega_c + \Omega_K^{th} + \Omega_N, \quad (8)$$

where Ω_c is the classical kaon contribution,

$$\Omega_c = V[-f^2 m_K^2 (\cos\langle\theta\rangle - 1) - 1/2 \cdot \mu_K^2 f^2 \sin^2\langle\theta\rangle], \quad (9)$$

and the thermal kaon contribution, is given as follows;

$$\Omega_K^{th} = TV \int \frac{d^3p}{(2\pi)^3} \ln(1 - e^{-\beta E_+(\mathbf{p})})(1 - e^{-\beta E_-(\mathbf{p})}). \quad (10)$$

It is to be noted that the zero-point-energy contribution of kaons is very small [16][17] and we discard it in this paper.

Ω_N denotes the nucleon contribution. In order to reproduce the bulk property of nuclear matter and get a realistic EOS for kaon condensation, we should take into account nucleon-nucleon interactions. Following Prakash et al.[18] we introduce the potential energy in the form,

$$E_N^{pot} = E_N^{sym} + E_N^V, \quad (11)$$

where E_N^{sym} represents the symmetry energy contribution and E_N^V the residual potential contribution. The symmetry energy is given by

$$E_N^{sym} = V \rho_B (1 - 2x)^2 S^{pot}(u); (u = \rho_B / \rho_0; \rho_0 = 0.16 \text{fm}^{-3}) \quad (12)$$

where the function $S^{pot}(u)$ reads,

$$S^{pot}(u) = (S_0 - (2^{2/3} - 1)(3/5)E_F^0)F(u) \quad (13)$$

with the constraint $F(u = 1) = 1$ to reproduce the empirical symmetry energy $S_0 \simeq 30 \text{MeV}$ at the nuclear density ρ_0 . E_F^0 is the fermi energy at ρ_0 . Hereafter we use $F(u) = u$ for an example. It is well-known that the nuclear symmetry energy, which stems from the kinetic and potential energies, plays an important role for the ground-state properties of the condensed phase. Since we have already included the kinetic energy for nucleons, we must take into account only the potential energy contribution, which should be beyond chiral dynamics.

On the other hand, as another potential contribution besides the symmetry energy we use the following formula which simulates the results given by sophisticated theoretical calculations[18],

$$E_N^V/V = \frac{1}{2}Au^2\rho_B + \frac{Bu^{\sigma+1}\rho_B}{1 + B'u^{\sigma-1}} + 3u\rho_B \sum_{i=1,2} C_i \left(\frac{\Lambda_i}{p_F^0} \right)^3 \left(\frac{p_F}{\Lambda_i} - \arctan \frac{p_F}{\Lambda_i} \right). \quad (14)$$

We choose the parameter set $(A, B, B', \sigma, C_i, \Lambda_i)$ for compression modulus to be $K_0 = 240 \text{ MeV}$ for normal nuclear matter ¹. Strictly speaking, the effective potential functions eqs.(12),(14) should include temperature dependence by way of the Pauli blocking effect on nucleon-nucleon scattering in matter. However, as has been shown in ref. [20] temperature-dependence should be weak up to several tens of MeV, so that we can use the form E_N^{pot} even at finite temperature.

Including the potential contribution E_N^{pot} , we get the single particle energies,

$$\begin{aligned}\epsilon_p(\mathbf{p}) &= \frac{p^2}{2M} - (\Sigma_{Kp} + \mu_K)(1 - \cos\langle\theta\rangle) + \frac{1}{V} \frac{\partial E_N^{pot}}{\partial \rho_p}, \\ \epsilon_n(\mathbf{p}) &= \frac{p^2}{2M} - (\Sigma_{Kn} + \mu_K/2)(1 - \cos\langle\theta\rangle) + \frac{1}{V} \frac{\partial E_N^{pot}}{\partial \rho_n}.\end{aligned}\quad (15)$$

We have used the nonrelativistic approximation for nucleons, where the scalar density is not distinguished from the ordinary density ρ_i .

Then nucleon contributions can be written in the form;

$$\Omega_N = \Omega_N^{kin} + \Omega_N^{pot}, \quad (16)$$

where Ω_N^{kin} is the “kinetic energy” contribution and Ω_N^{pot} the “potential energy” contribution,

$$\begin{aligned}\Omega_N^{kin} &\simeq -2TV \sum_{n,p} \int \frac{d^3p}{(2\pi)^3} \ln(1 + e^{-\beta(\epsilon_i(\mathbf{p}) - \mu_i)}), \\ \Omega_N^{pot} &= -\rho_B \frac{\partial E_N^{pot}}{\partial \rho_B}.\end{aligned}$$

Here it is useful to introduce the new parameters $\mu_i^0 (i = n, p)$ instead of the chemical potentials μ_i ,

$$\begin{aligned}\mu_p^0 &= \mu_p + (\mu_K + \Sigma_{Kp})(1 - \cos\langle\theta\rangle) - \frac{1}{V} \frac{\partial E_N^{pot}}{\partial \rho_p}, \\ \mu_n^0 &= \mu_n + \left(\frac{\mu_K}{2} + \Sigma_{Kn}\right)(1 - \cos\langle\theta\rangle) - \frac{1}{V} \frac{\partial E_N^{pot}}{\partial \rho_n}.\end{aligned}\quad (17)$$

¹Since this parameter set has been also used in Ref.[19] in which $V(u)$ corresponds to our expression E_N^V , our results at zero-temperature are the same as theirs.

Then Ω_N^{kin} can be written in the simple form,

$$\Omega_N^{kin} \simeq -2TV \sum_{n,p} \int \frac{d^3p}{(2\pi)^3} \ln(1 + e^{-\beta(\epsilon^0(\mathbf{p}) - \mu_i^0)}), \quad (18)$$

with the “free” kinetic energy $\epsilon^0(\mathbf{p}) = p^2/2M$.

Using the thermodynamic relations,

$$S_{chiral} = -\frac{\partial \Omega_{chiral}}{\partial T}, \quad Q_i = -\frac{\partial \Omega_{chiral}}{\partial \mu_i}, \quad E_{chiral} = \Omega_{chiral} + TS_{chiral} + \sum \mu_i Q_i, \quad (19)$$

we can find charge, entropy and internal energy. The entropy is given by

$$\begin{aligned} S_{chiral} = & -\beta \Omega_{chiral} + \beta V f^2 \left(-\frac{1}{2} \mu_K^2 \sin^2 \langle \theta \rangle + m_K^2 (1 - \cos \langle \theta \rangle) \right) \\ & + \beta V \int \frac{d^3p}{(2\pi)^3} [E_-(\mathbf{p}) f_B(E_-(\mathbf{p})) + E_+(\mathbf{p}) f_B(E_+(\mathbf{p}))] \\ & + 2\beta V \sum_{n,p} \int \frac{d^3p}{(2\pi)^3} [(\epsilon^0(\mathbf{p}) - \mu_i^0) f_F(\epsilon^0(\mathbf{p}) - \mu_i^0)] \\ & - \beta V (1 - 2x)^2 S^{pot}(u) \rho_B, \end{aligned} \quad (20)$$

with the Fermi-Dirac distribution function $f_F(E)$ and the Bose-Einstein distribution function $f_B(E)$. The kaonic charge is given by,

$$Q_K = V \left[\mu_K f^2 \sin^2 \langle \theta \rangle + \cos \langle \theta \rangle n_K + (1 + x) \sin^2(\langle \theta \rangle / 2) \rho_B \right], \quad (21)$$

with the number density n_K of thermal kaons,

$$n_K = \int \frac{d^3p}{(2\pi)^3} [f_B(E_-(\mathbf{p})) - f_B(E_+(\mathbf{p}))]. \quad (22)$$

Nucleon charges are given by

$$Q_i = 2V \int \frac{d^3p}{(2\pi)^3} [f_F(\epsilon^0(\mathbf{p}) - \mu_i^0)], \quad (i = n, p). \quad (23)$$

Then the total energy is given by

$$E_{chiral} = V f^2 \left(-\frac{1}{2} \mu_K^2 \sin^2 \langle \theta \rangle + m_K^2 (1 - \cos \langle \theta \rangle) \right)$$

$$\begin{aligned}
& + V \int \frac{d^3p}{(2\pi)^3} [E_-(\mathbf{p})f_B(E_-(\mathbf{p})) + E_+(\mathbf{p})f_B(E_+(\mathbf{p}))] \\
& + 2V \sum_{n,p} \int \frac{d^3p}{(2\pi)^3} \left[\left(\epsilon_i(\mathbf{p}) - \frac{1}{V} \frac{\partial E_N^{pot}}{\partial \rho_n} \right) f_F(\epsilon^0(\mathbf{p}) - \mu_i^0) \right] \\
& + V(1-2x)^2 S^{pot}(u) \rho_B + \mu_K Q_K,
\end{aligned} \tag{24}$$

where we add the term with $\frac{1}{V} \frac{\partial E_N^{pot}}{\partial \rho_n}$, to avoid double-counting.

The total thermodynamic potential Ω_{total} is given by adding the one for leptons (electrons, muons and neutrinos), Ω_l , $\Omega_{total} = \Omega_{chiral} + \Omega_l$;

$$\Omega_l = -2TV \sum_{e,\mu,\nu} \int \frac{d^3p}{(2\pi)^3} \left[\ln(1 + e^{-\beta(\epsilon_i(\mathbf{p}) - \mu_i)}) + \ln(1 + e^{-\beta(\epsilon_{\bar{i}}(\mathbf{p}) + \mu_i)}) \right], \tag{25}$$

with $\epsilon_i(\mathbf{p}) = \epsilon_{\bar{i}}(\mathbf{p}) = \sqrt{m_i^2 + p^2}$ ($i = e, \mu, \nu_e, \nu_\mu$).

The parameters $x, \langle \theta \rangle$ and chemical potentials μ_K, μ_i ($i = n, p$) are determined by the extremum conditions for given density and temperature. The first condition demands $\partial \Omega_{total} / \partial x = 0$, which is equivalent with the condition for chemical equilibrium among kaons, nucleons:

$$\mu_n - \mu_p = \mu_K, \tag{26}$$

or

$$\mu_p^0 - \mu_n^0 - 4S^{pot}(u)(1-2x) + \frac{1 - \cos \langle \theta \rangle}{2} \{ 2(\Sigma_{Kn} - \Sigma_{Kp}) - \mu_K \} + \mu_K = 0, \tag{27}$$

by way of Eq. (17). The charge neutrality demands $\partial \Omega_{total} / \partial \mu_K = 0$:

$$Q_K + Q_e + Q_\mu = Q_p (= xV\rho_B), \tag{28}$$

where the hadron charges are given in Eqs. (21),(23) and the lepton numbers are given by

$$Q_i \equiv Y_i \rho_B = 2V \int \frac{d^3p}{(2\pi)^3} [f_F(\epsilon_i(\mathbf{p}) - \mu_i) - f_F(\epsilon_{\bar{i}}(\mathbf{p}) + \mu_i)], \tag{29}$$

with the lepton-number fractions Y_i ($i = e, \mu$). Finally the extremum condition with respect to $\langle \theta \rangle$ gives

$$0 = f^2 \sin \langle \theta \rangle (m_K^{*2} - 2\mu_K b - \mu_K^2 \cos \langle \theta \rangle) + \frac{\partial(\Omega_K/V)}{\partial \langle \theta \rangle}, \tag{30}$$

which is just the field equation of kaon at momentum zero. Eqs. (27),(28), (30) are the basic equations to determine the equilibrated state.

We can see that once the fluctuation contribution (the second term in Eq.(30)) is taken into account, the relation $E_-(\mathbf{p} = 0) = 0$ no longer holds. So the Goldstone nature is violated up to one-loop order in the loop expansion. This situation always occurs in the perturbation theory [21]: the number of loops are *always* different between the thermodynamic potential (N_l) and the self-energy for kaons ($N_l - 1$). This shortcoming is never cured unless we perform a full order calculation. This matter is beyond the scope of this paper. Fortunately, the contribution of fluctuations can be estimated to be small in the temperature-density region we are interested in[13].

3 Numerical Results and Discussions

Using the formulation given in Sect.2, we study the properties of kaon condensed matter taking into account thermal and neutrino-trapping effects and then discuss the properties of PNS. Finally some implications on the delayed collapse of PNS will be given.

3.1 Phase Diagram

First we show the phase diagram in Fig.1 for neutrino-free and trapping matter. In the neutrino-trapping case, there exist additional conditions with respect to the conservation of lepton numbers[19]. Recent calculations of gravitational core collapse of massive stars indicate the electron lepton number Y_{le} at the onset of neutrino-trapping $Y_{le} \approx 0.35$ [22].

Then we take $Y_{le} \equiv Y_e + Y_{\nu_e} = 0.4$ and 0.3 and for muon $Y_{l\mu} \equiv Y_\mu + Y_{\nu_\mu} = 0.0$ in the neutrino-trapping case. On the other hand, in the neutrino-free case, $Y_{\nu_e} = Y_{\nu_\mu} = 0$.

In the phase diagram the temperature-density plane is separated into two regions by the critical line; the left-side region means normal phase, and the right-side region the kaon-condensed phase. We can see that both of the neutrino-trapping and thermal effects work against the phase transition. In the low-temperature case the neutrino trapping effect is dominant, while both effects become comparable at high-temperature.

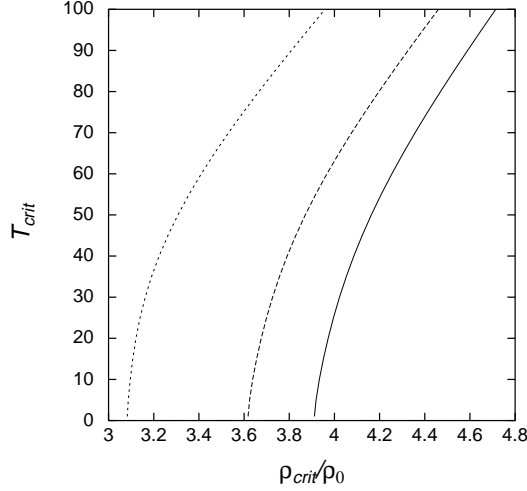


Figure 1: Phase Diagram: solid line and dashed line are for the neutrino-trapped cases, $Y_{le} = 0.4$ and 0.3 , respectively and dotted line for the neutrino-free case.

The neutrino-trapping effect may be simply understood as follows. Kaon condensation occurs when the lowest kaon energy (ϵ_{K^-}) is equal to kaon chemical potential (μ_K): ϵ_{K^-} decreases by strongly attractive kaon-nucleon interactions as density increases, while $\mu_K = \mu_n - \mu_p$ increases to match ϵ_{K^-} at the critical density. In the neutrino-trapping case, the chemical equilibrium due to weak interactions implies that the relation, $\mu_K = \mu_n - \mu_p = \mu_e - \mu_{\nu_e}$, holds. Compared with the neutrino-free case $\mu_{\nu_e} = 0$, μ_K should be reduced due to the finite contribution of μ_{ν_e} . Hence higher density is needed to satisfy the matching condition.

3.2 EOS for thermal and isentropic matter

Here we compare the EOS for the two cases: the isothermal and isentropic cases. EOS under the isothermal condition ($T = 0, 40$ and 80 MeV) for kaon condensed matter and normal matter is depicted in Fig.2. The resulting EOS for kaon condensed matter shows the existence of the thermodynamically unstable region because the phase transition is of first order and large softening

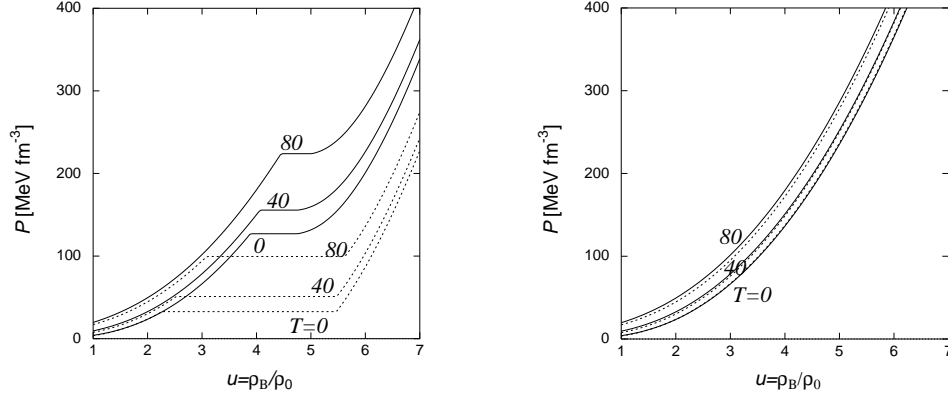


Figure 2: Pressure of isothermal matter ($T = 0, 40$ and 80MeV) for kaon condensed matter[left panel] and for normal matter[right panel]. Solid lines and dashed lines are for the neutrino-trapped case ($Y_{le} = 0.4$) and the neutrino-free case, respectively.

of EOS so that we have recourse to the Maxwell construction to obtain the realistic EOS in equilibrium². There appears the equi-pressure region as a result of the Maxwell construction. We can see that both the thermal and neutrino-trapping effects stiffen the EOS mainly through the suppression of kaon condensate. Then, in comparison of EOS for normal matter, the thermal effect is profound in particular around the critical density.

The equi-pressure region becomes narrower as temperature increases or neutrinos are trapped more, which implies that the magnitude of the first-order phase transition is reduced by both effects by temperature and neutri-

²Strictly speaking, we need to apply the Gibbs condition. Recently an attempt to drive a realistic EOS along this line appeared[23][24]. Then EOS should be smoothed due to the appearance of the mixed phase, where the normal matter and the kaon condensed matter coexist. At the beginning of the mixed phase, matter is expected to contain droplets of, negatively charged, kaon-condensed matter embeded in, positively charged, normal matter. However it seems to be difficult to take into account the surface and Coulomb energies of the droplets properly; generally speaking these effects tend to suppress the existence of the mixed phase. Furthermore, some works suggest that sometimes the Gibbs condition cannot be satisfied [14][25]. So we leave this matter for a future study and use here the Maxwell construction for simplicity to get the EOS in equilibrium and discuss the characteristics due to the Maxwell construction in Appendix A.

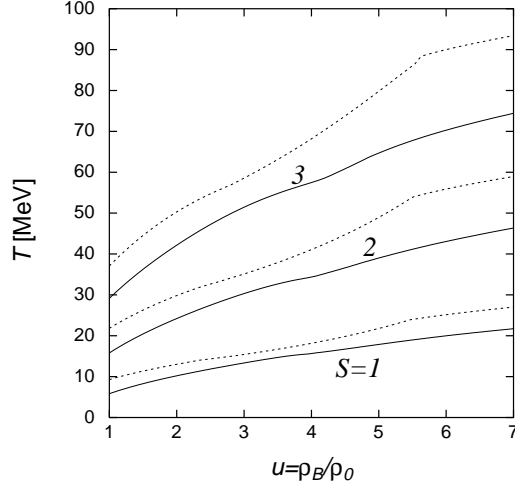


Figure 3: Isentropic lines: $S = 1, 2, 3$ solid lines and dashed lines are for the neutrino-trapped case ($Y_{le} = 0.4$), the neutrino-free case, respectively

nos. We can see the remarkable narrowness, especially in neutrino-trapping condition because trapped neutrinos suppress not only the occurrence of kaon condensation but also the growth of the condensate. We shall see later that the existence of the equi-pressure region induces the gravitationally unstable region in the branch of neutron stars.

For the isentropic case, which might be more relevant for PNS matter, we find the temperature profile as a function of density by the use of eq.(20) and lepton contribution. We show the isentropic line in density-temperature plane in Fig.3. Under the isentropic condition in which entropy per baryon (S) is taken constant (1,2 or 3) over the star interior, temperature increases as density becomes high. This means that once we construct a neutron star with isentropic matter, temperature becomes the highest at the center of the star.

The isentropic EOS can be obtained by connecting the values of pressure at the corresponding temperatures for given densities (Fig.4). It is to be noted that the equi-pressure region, under the isentropic condition, disappears except for the $S = 0$ case.

It is well known that when the equi-pressure region exists in the EOS,

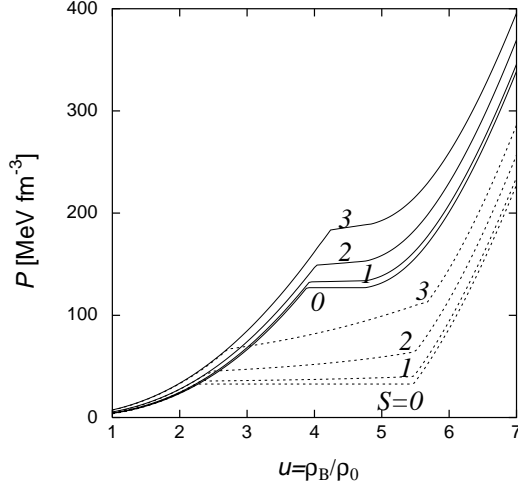


Figure 4: Pressure for isentropic matter ($S = 0, 1, 2, 3$). Solid line and dashed line for neutrino-trapping case ($Y_{le} = 0.4$) and neutrino-free case respectively.

neutron star also has a density gap[26]. In the isentropic case, the equilibrium region no longer exists and the density gap disappears even if we apply the Maxwell construction for the isothermal EOS. Instead the mixed phase appears inside the neutron star³.

3.3 Properties of PNS and possibility of the delayed collapse

Using the isentropic EOS, we construct PNS by solving TOV equation. In Fig.5 we show the central density-gravitational mass relation for the neutrino-free or -trapping cases with entropy per baryon $S = 0, 1, 2$ or 3 . We can see thermal effect is large for the stars whose central density is around the critical density because of the obvious stiffness of the pressure in this region. On the other hand, mass of the stars with high central density seems not to be so changed by thermal effect. This is because thermal effect causes not only

³Note that this mixed phase should be distinguished from the one resulted from the Gibbs condition.

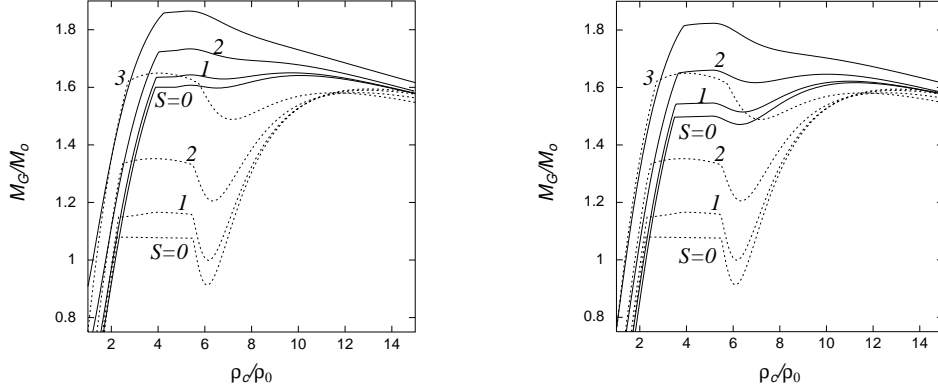


Figure 5: Central density versus gravitational mass. Solid lines and dashed lines for neutrino-trapping ($Y_{le} = 0.4$ [left panel] or $Y_{le} = 0.3$ [right panel]) and neutrino-free PNS respectively at $S = 0, 1, 2, 3$.

higher pressure but also larger energy which in turn results in the stronger gravity. Sometimes this leads to the lower maximum mass at the higher entropy.

We can find that, clearly in the neutrino-free case, once kaon condensation occurs in the core of a star, gravitationally unstable region (negative gradient part) appears and the neutron-star branch is separated into two stable branches: one is for stars with kaon condensate in their cores and the other consisting of only normal matter. The maximum mass, stars with which include kaon condensate in the core, is hardly changed but decreases by the thermal effect because of the strong gravity except $S = 3$ case.

In the neutrino-trapping cases, for $S = 0$ or 1 , we can see that the neutron-star branch is also separated by the gravitaionally unstable region and the maximum mass lies on the branch with kaon condensate.

On the other hand, in other cases: $S = 3$ in neutrino-free, $S = 2, 3$ in neutrino-trapping, almost all of the stars with kaon condensate are gravitationally unstable, and the maximum-mass star still resides on the normal branch. For this reason the central density of the maximum-mass star is very different from those for $S = 0$ or 1 . In table 1 we summarize the data for stars with maximum mass in each case. We can easily expect that there is a

	branch	central density	gravitational mass	total baryon number
ν -free $Y_{\nu_e} = 0$				
$S = 0$	K	$13.2\rho_0$	$1.59M_\odot$	2.24×10^{57}
$S = 1$	K	$13.5\rho_0$	$1.59M_\odot$	2.22×10^{57}
$S = 2$	K	$12.5\rho_0$	$1.58M_\odot$	2.14×10^{57}
$S = 3$	N	$4.0\rho_0$	$1.65M_\odot$	2.11×10^{57}
ν -trapping $Y_{le} = 0.4$				
$S = 0$	K	$10.0\rho_0$	$1.64M_\odot$	2.13×10^{57}
$S = 1$	K	$9.6\rho_0$	$1.65M_\odot$	2.14×10^{57}
$S = 2$	N	$5.4\rho_0$	$1.73M_\odot$	2.23×10^{57}
$S = 3$	N	$5.3\rho_0$	$1.86M_\odot$	2.36×10^{57}
ν -trapping $Y_{le} = 0.3$				
$S = 0$	K	$11.3\rho_0$	$1.62M_\odot$	2.15×10^{57}
$S = 1$	K	$11.0\rho_0$	$1.62M_\odot$	2.14×10^{57}
$S = 2$	N	$5.1\rho_0$	$1.66M_\odot$	2.15×10^{57}
$S = 3$	N	$5.1\rho_0$	$1.82M_\odot$	2.33×10^{57}

Table 1: Configuration for stars with maximum mass: which branch the star resides in, normal branch(N) or kaon condensed branch(K), its central density, mass and total baryon number.

critical value of entropy for which the star begins to take the maximum mass on the normal branch.

To discuss the possibility of the delayed collapse of PNS, the total baryon number N_B should be fixed as a conserved quantity during the evolution [27] under the assumption that there is no accretion in the deleptonization and initial cooling stages.

Discarding gravitationally unstable stars, we show mass of stable stars for given baryon numbers in Fig.6. Each terminal point represents maximum mass and maximum total baryon number in each condition. If initial mass is beyond the terminal point when the neutron star is born, it should collapse into a black hole (not a delayed collapse but an usual formation of a black hole during supernova explosion). We have shown the neutrino-trapping and -free cases; the former case corresponds to the initial stars before the deleptonization era, while the latter to the initial cooling era after deleptonization.

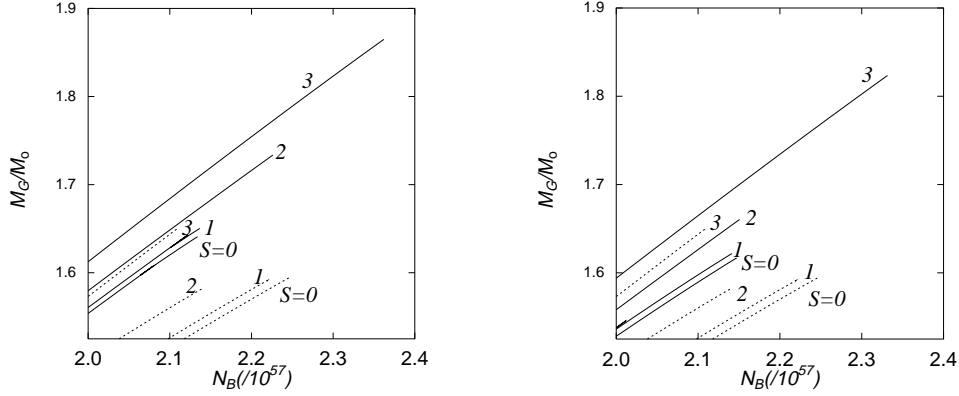


Figure 6: Total baryon number and gravitational mass for stable PNS. Solid lines and dashed lines for neutrino-trapping ($Y_{le} = 0.4$ [left panel] or $Y_{le} = 0.3$ [right panel]) and neutrino-free PNS, respectively at $S = 0, 1, 2, 3$.

It is interesting to see the difference between the neutrino-free and trapping cases: the curve is shortened as the entropy increases in the former case, while elongated in the latter case. The difference comes from which branch the maximum mass star resides in. These features are responsible for the following discussion about the delayed collapse and maximum mass of the cold neutron stars.

The delayed collapse takes place if the initially stable star on a curve finds no corresponding stable point on other curves at any stage in its evolution through deleptonization or cooling. When we discuss the evolution, several timescales are important: t_K for the onset and growth of kaon condensation, t_{del} and t_{cool} for deleptonization and initial cooling, respectively. However we can neglect t_K because $t_K \ll$ several sec. $\approx t_{del} < 20\text{-}30$ sec. $\approx t_{cool}$ [1][28].

Now, consider the typical evolution for example: PNS have initially $Y_{le} = 0.4$ and $S = 2$ after supernova explosion and evolve through deleptonization into neutrino-free and $S = 2$ stage as an intermediate stage. We can see clearly the PNS with $1.68M_\odot \leq M_G \leq 1.73M_\odot$ can exist as meta-stable stars at the beginning but cannot find any point on the neutrino-free and $S = 2$ curve. Therefore they must collapse to the low-mass black holes in the deleptonization era. It is to be noted that because the $Y_{le} = 0.4$ and $S = 2$

stars hardly include kaon condensate, their collapse are largely due to the appearance of kaon condensate in its core.

Furthermore we can also determine the maximum mass of cold neutron stars by taking into account the evolution of PNS, as an extension from the previous work in neutrino-free case[27]. Usually we assign the maximum mass of cold neutron stars as the terminal point on the line in neutrino-free and $S = 0$ configuration in Fig.6 ($M_{max} = 1.59M_{\odot}$). However, it is wrong when we take into account the evolution of neutron stars, especially in the initial cooling stage. In order to see how to determine the realistic maximum mass of the cold neutron stars, we consider a typical evolution with total baryon number fixed. With the evolution we have already adopted, stars with total baryon number more than the terminal point of $S = 2$ and neutrino-free line should collapse to black-holes in the deleptonization era and cannot evolve stably to usual cold neutron stars. Therefore only stars with the total baryon number $N_B \leq 2.14 \times 10^{57}$ can evolve to cold neutron stars and the corresponding maximum mass is $1.54M_{\odot}$ (See Fig.6 and Table 1). Generally speaking, maximum mass should be determined by taking into account the evolution. In our calculation it seems that not the neutrino trapping stage but the neutrino free and hot stage plays an important role to determine the maximum mass.

If we assume other scenarios, we can of course determine the maximum mass of cold neutron stars and stars which should collapse to the low mass black hole in each case.

We can conclude that the delayed collapse possibly takes place in the deleptonization era due to the occurrence of kaon condensation and maximum mass cannot be determined in the evolution by the deleptonization but by the initial cooling era.

Next, we show that the delayed collapse in case of normal matter (without any phase transition) is impossible. In Fig.7 gravitational mass for gravitationally stable *normal* neutron stars is plotted as a function of total baryon number N_B . Each terminal point represents the maximum mass star in each configuration. Similarly to the above discussion, we can study stability of neutron stars in the deleptonization or cooling stage. After all every star can find the stable point in each stage, and the delayed collapse of *normal* neutron stars is impossible from the static argument.

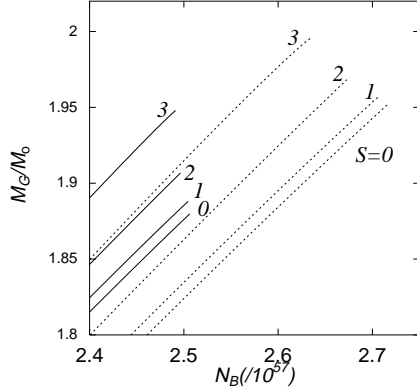


Figure 7: Total baryon number and gravitational mass for normal matter. Solid lines and dashed lines for neutrino-trapping ($Y_{le} = 0.4$) and neutrino-free PNS, respectively at $S = 0, 1, 2, 3$.

4 Summary and Concluding Remarks

In this paper, using our framework to treat the kaon condensation based on chiral symmetry, we have discussed its implication on astrophysics, the delayed collapse. When we neglect any phase transition, the delayed collapse is impossible neither in deleptonization nor in cooling stage. On the other hand, when kaon condensation is realized, the delayed collapse is possible in the deleptonization stage. We insist that not the thermal effects but the effect of trapped neutrinos give rise to the delayed collapse under no accretion of matter from the surroundings. This point is a main difference to the previous work about kaon condensation and the delayed collapse[14].

In order to study the mechanism of the delayed collapse and mass region of PNS to collapse in more detail, we have to study the dynamical evolution beyond the static discussion given here. The accretion of a fall-back mass may be an important ingredient[3][4][5], by which the delayed collapse may occur more easily. Neutrino opacity is another important ingredient in that study; We must treat the change of EOS and neutrino opacity in a consistent way. Since the neutrino-nucleon scattering or neutrino absorption should be enhanced in the kaon condensed phase[24][29] the neutrino-trapping era might last longer.

As another remaining issue, the extension of EOS is also important. In this paper we have applied the Maxwell construction. We will discuss the EOS in equilibrium using the Gibbs condition, which make our conclusion firmer. However, we believe our main conclusion will not be changed so much because modification by the Gibbs condition seems to give little effects for light neutron stars (See Appendix A). Moreover we will include the effects of thermal kaon's loops on the nucleon propagator and zero-point energy[13][12].

Our conclusion depends on the behavior of EOS. In this paper we considered the kaon condensation and the suppression of condensate due to the trapping neutrinos is a key object to conclude that the delayed collapse is possible. It is very interesting to study other phase transitions, for example, quark matter[30] and discuss whether the delayed collapse is possible or not, which may become one candidate to distinguish what kind of matter exists in the core of neutron stars.

5 Acknowledgement

We thank T. Harada, K. Nakao, T. Takatsuka and T. Muto for useful discussions and comments.

This work was supported in part by the Research Fellowships of the Japan Society for the Promotion of Science for Young Scientists and by the Japanese Grant-in-Aid for Scientific Research Fund of the Ministry of Education, Science, Sports and Culture(11640272).

Appendix A

In this paper we have applied the Maxwell construction to get the EOS in equilibrium. Here, we discuss some features due to the Maxwell construction.

We show the neutron stars at $T = 0$ in Fig.8(also see Fig.2). Typical

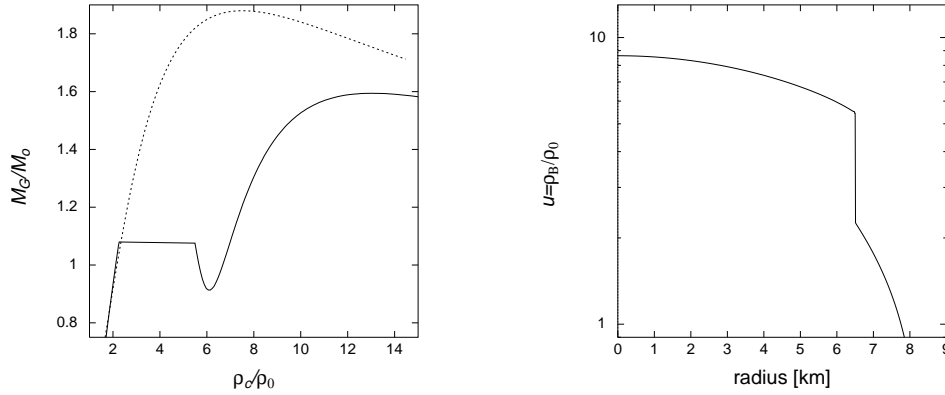


Figure 8: [left panel] Central density versus gravitational mass. Solid lines and dashed lines for neutron stars at $T = 0$ with kaon condensed matter and normal matter. [right panel] Structure of a neutron star with kaon condensed matter and with $M = 1.4M_\odot$.

characteristics are found as follows:

1. Gravitaionally unstable region ($\partial M_G/\partial \rho_c < 0$) appears.(left panel)
2. There is no coexisting phase.(right panel)
3. Density gap exists : $2.27 < \rho/\rho_0 < 5.47$.(left panel)

Though these features will disappear when we apply the Gibbs condition to the EOS[23]. The behavior of the neutron stars(both solid lines) will be smoothed and bulk properties will not be changed so much. The differences in the bulk properties of neutron stars (gravitational mass, radius and so on) between the Maxwell construction and the Gibbs condition are mainly profound for stars with small mass, while they should be small for heavy neutron stars[23]. Our discussion in this paper are based on the Maxwell construction and when we use more realistic EOS details of our conclusion may be modified. However the Maxwell construction seems not to change

our main conclusion that the neutrino-trapping effects play an important role of the scenario of the delayed collapse.

References

- [1] M. Prakash, I. Bombaci, M. Prakash, P. J. Ellis, J. M. Lattimer and R. Knorren, Phys. Rep. **280** (1997) 1.
- [2] G. E. Brown and H. A. Bethe, Astrophys. J. **423** (1994) 659.
- [3] S.E. Woosley and F.X. Timmers, Nucl. Phys. **A606** (1996) 137.
- [4] L. Zampieri, M. Colpi, S.L. Shapiro and I. Wasserman, Astrophys. J. **505** (1998) 876.
- [5] C.L. Fryer, S.L. Colgate and P.A. Pinto, Astrophys. J. **511** (1999) 885.
- [6] T.W. Baumgarte, S.L. Shapiro and S. Teukolsky, Astrophys. J. **443** (1996) 680.
- [7] W. Keil and H.-Th. Janka, Astron. and Astrophys. **296** (1995) 145.
- [8] J.A. Pons, S. Reddy, M. Prakash, J.M. Lattimer and J.A. Miralles, *astro-ph/9807040*.
- [9] D.B. Kaplan and A.E. Nelson, Phys. Lett. **B175** (1986) 57; **B179** (1986) 409(E).
- [10] For review article, C.-H. Lee, Phys. Rep. **275** (1996) 255.
- [11] T. Tatsumi and M. Yasuhira, Phys. Lett. **B441** (1998) 9.
- [12] M. Yasuhira and T. Tatsumi, in *Physics of Hadrons and QCD*, edited by H. Yabu, K. Itakura, T. Matsui and M. Oka (World Scientific 1999), pp248-251.
- [13] T. Tatsumi and M. Yasuhira, Nucl. Phys. **A653** (1999) 133.
- [14] J.A. Pons, S. Reddy, P.J. Ellis, M. Prakash and J.M. Lattimer, *nucl-th/0003008*.
- [15] J. Gasser and H. Leutwyler, Phys. Lett. **B188** (1987) 477.
F.C. Hansen, Nucl. Phys. **B345** (1990) 685.
- [16] V. Thorsson and P.J. Ellis, Phys. Rev. **D55** (1997) 5177.

- [17] M. Yasuhira and T. Tatsumi, in preparation.
- [18] M. Prakash, T.L. Ainsworth and J.M. Lattimer, Phys. Rev. Lett. **61**, 2518 (1988).
- [19] V. Thorsson, M. Prakash, J.M. Lattimer Nucl. Phys. **A572** (1994) 693.
- [20] T. Takatsuka and J. Hiura, Prog. Theor. Phys. **79** (1988) 268.
- [21] J.I. Kapusta, *Finite-temperature field theory* (Cambridge U. Press, Cambridge, 1989).
- [22] R.I. Epstein and C.J. Pethick, Astrophys. J. **243** (1981) 243.
- [23] N.K. Glendenning and J. Schaffner-Bielich, Phys. Rev. Lett. **81** (1998) 4564; Phys. Rev. **C60** (1999) 025803.
- [24] S. Reddy, G. Bertsch and M. Prakash, Phys. Lett. **B475** (2000) 1.
- [25] H. Heiselberg, C.J. Pethick, and E.F. Staubo, Phys. Rev. Lett. **70** (1993) 1355.
- [26] H. Fujii, T. Maruyama, T. Muto and T. Tatsumi, Nucl. Phys. **A597** (1996) 645.
- [27] T. Takatsuka, Prog. Theor. Phys. **95** (1996) 901.
- [28] T. Muto, T. Tatsumi and N. Iwamoto, Phys. Rev. **D61** (2000) 063001; Phys. Rev. **D61** (2000) 083002.
- [29] T. Muto, T. Tatsumi, N. Iwamoto and M. Yasuhira, in preparation.
- [30] For review article, J. Madsen, *astro-ph/9809032*.